


Optical Magnetism and Huygens' Surfaces in Arrays of Atoms Induced by Cooperative Responses

K. E. Ballantine^{✉*} and J. Ruostekoski^{✉†}

Department of Physics, Lancaster University, Lancaster LA1 4YB, United Kingdom

 (Received 28 February 2020; accepted 31 August 2020; published 2 October 2020)

By utilizing strong optical resonant interactions in arrays of atoms with electric dipole transitions, we show how to synthesize collective optical responses that correspond to those formed by arrays of magnetic dipoles and other multipoles. Optically active magnetism with the strength comparable with that of electric dipole transitions is achieved in collective excitation eigenmodes of the array. By controlling the atomic level shifts, an array of spectrally overlapping, crossed electric and magnetic dipoles can be excited, providing a physical realization of a nearly reflectionless quantum Huygens' surface with the full 2π phase control of the transmitted light that allows for extreme wavefront engineering even at a single photon level. We illustrate this by creating a superposition of two different orbital angular momentum states of light from an ordinary input state that has no orbital angular momentum.

DOI: [10.1103/PhysRevLett.125.143604](https://doi.org/10.1103/PhysRevLett.125.143604)

A crucial limitation for utilizing atoms as optical media is the inability of light to couple to atoms using both its electric and magnetic components. Optical magnetic dipole transitions in atoms typically are very weak to the extent that magnetic susceptibility at optical frequencies has generally been considered a meaningless concept [1], and the optical response is determined by strong oscillating electric dipoles [2]. The absence of magnetic coupling in natural media has led to the development of artificial metamaterials [3] and metasurfaces [4], representing man-made designer materials that simultaneously provide strong interactions with both field components of light [5]. The quest for dramatic consequences of this from perfect lensing [6] to invisibility cloaks [7–9] has been driving the development, but performance at optical frequencies has been limited.

Here we show that strong light-mediated interactions between cold atoms in planar arrays can be designed to synthesize *collective* radiative excitations that exhibit strong electric and magnetic optical responses. The system has considerable advances over artificial fabricated materials because of the absence of dissipative losses due to absorption and the possibility to reach the quantum regime in the optical manipulation and control. We illustrate the flexibility of designing collective radiative excitations by proposing a Huygens' surface of atoms, where the crossed electric and magnetic dipolar resonances act as elementary sources for wave propagation according to Huygens' principle [10,11]. Huygens' principle then states that an *arbitrary* wavefront can be constructed by an ideal physical realization of a Huygens' surface, therefore achieving extreme optical manipulation. In a single-photon limit, our proposed array provides a quantum-photonics

wave-engineering tool, with beam shaping, steering, and focusing capabilities.

Atomic physics technology provides a variety of approaches for trapping closely spaced atoms in arrays with single-site control and unit occupancy per site [12–18]. For cold atoms with subwavelength spacing, the light-mediated interactions can be very strong due to resonant light undergoing multiple scattering between the atoms [19–43], when the realization of strong collective coupling in large resonator arrays of metasurfaces typically requires special arrangements [44,45]. Moreover, the atomic arrays can offer a promising platform for quantum information processing at the level of single photon excitations [29,46,47]. Experiments on strong collective optical responses of trapped cold atomic ensembles are actively ongoing [48–61], and the first measurements of the transmitted light through an optical lattice of atoms in a Mott-insulator state have now been performed [62] that demonstrate subradiant resonance narrowing where the entire lattice responds as a coherent collective entity.

Here we propose to engineer strong resonant dipole-dipole interactions by design atomic arrays, such that each unit cell of the periodic lattice, consisting of a small number of sites, has a specific symmetry that characterizes the collective excitation eigenmodes of the array. The modes extend over the entire sample and in large lattices the effect of the light-mediated interactions becomes strong, even when radiation rates of an individual unit cell are closer to those of an isolated atom. This allows us to utilize strongly subradiant collective eigenmodes, with suppressed emission rates, as weakly radiating “dark” states. We use the dark states to synthesize optically active magnetism via an

array of magnetic dipoles that can indirectly be excited by incident light.

We show that collective resonances can be superposed to form an array of electric and magnetic dipoles. Together with the control of the full 2π phase coverage of transmitted light with almost no reflection, this realizes a Huygens' surface for light. Wavefront engineering is illustrated by transforming a Gaussian wave to a superposition of orbital angular momentum (OAM) beams with differing OAM. In the single-photon limit, such entangled OAM states can provide a useful resource for quantum information [63] that is not limited to two-state systems [64]. Physical implementations of Huygens' surfaces in weakly interacting metamaterials have been achieved in metallic systems using microwaves [65], but optical frequencies pose severe challenges, e.g., due to absorption and lack of suitable magnetic resonances. Near-infrared or optical Huygens' sources or closely related metasurface controls have been realized using dielectric nanoparticles [66–71].

The atoms are confined in a 2D lattice in the yz plane with one atom per site. We consider a $J = 0 \rightarrow J' = 1$ transition with a controllable Zeeman splitting of the $J' = 1$ levels, which could be achieved with ac Stark shifts of lasers or microwaves [72] or magnetic fields. The formalism we employ can describe the dynamics of two different regimes. The first is the decay of a single-photon excitation spread across the lattice, described by the density matrix $\rho = |\psi\rangle\langle\psi| + p_g|G\rangle\langle G|$ where p_g is the probability that the excitation has decayed, $|G\rangle$ is the state with all atoms in the ground state, and single-excitation states are represented by $|\psi\rangle = \sum_{j,\nu} \mathcal{P}_\nu^{(j)}(t) \hat{\sigma}_{j\nu}^+ |G\rangle$ [73]. Here $\hat{\sigma}_{j\nu}^+$ is the raising operator from the ground state to the excited state ν on atom j [46,47,83,84]. Such a single-photon excitation could be initialized by short-range coupling to a control qubit, e.g., using laser-assisted coupling between Rydberg states [46].

The same dynamics (when only considering one-body expectation values) also describes the classical polarization amplitudes of each atomic dipole in the limit of low drive intensity [85–90]. The dipole moment of atom j for the transitions $|J = 0, m = 0\rangle \rightarrow |J' = 1, m = \sigma\rangle$ is $\mathbf{d}_j = \mathcal{D} \sum_\sigma \hat{\mathbf{e}}_\sigma \mathcal{P}_\sigma^{(j)}$, where \mathcal{D} denotes the reduced dipole matrix element, $\mathcal{P}_\sigma^{(j)}$ the polarization amplitudes, and $\hat{\mathbf{e}}_\sigma$ unit polarization vectors [73]. In this case, the atoms are typically driven by a laser. We take an incident light field as $\mathcal{E}(r) = \mathcal{E}_0(y, z) \hat{\mathbf{e}}_y \exp(ikx)$ [91].

In a vector form $\mathbf{b}_{3j-1+\sigma} = \mathcal{P}_\sigma^{(j)}$, the collective response of atoms then results from a linear set of coupled equations due to the driving by the incident light, $\mathbf{F}_{3j-1+\sigma} = i\xi \hat{\mathbf{e}}_\sigma^* \cdot \epsilon_0 \mathcal{E}(\mathbf{r}_j) / \mathcal{D}$ where $\xi = 6\pi\gamma/k^3$ is given in terms of the single atom linewidth $\gamma = \mathcal{D}^2 k^3 / (6\pi\hbar\epsilon_0)$, and the scattered light from all the other atoms, such that $\dot{\mathbf{b}} = i\mathcal{H}(\mathbf{b} + \mathbf{F})$ [73,74]. The matrix \mathcal{H} has diagonal elements $\Delta_\sigma^{(j)} + i\gamma$, where $\Delta_\sigma^{(j)}$ is the detuning of level $m = \sigma$ from resonance with the driving frequency ω . The off-diagonal elements

correspond to dipole-dipole coupling between atoms $\xi \hat{\mathbf{e}}_\sigma^* \cdot \mathbf{G}(\mathbf{r}_j - \mathbf{r}_l) \hat{\mathbf{e}}_\sigma$, for $j \neq l$, where \mathbf{G} denotes the dipole radiation kernel, such that $\epsilon_0 \mathbf{E}_s^{(l)}(\mathbf{r}) = \mathbf{G}(\mathbf{r} - \mathbf{r}_l) \mathbf{d}_l$ gives the scattered field at \mathbf{r} from the atom l at \mathbf{r}_l [73,75]. The response can then be understood in terms of the collective eigenmodes \mathbf{v}_n of non-Hermitian \mathcal{H} [76], with corresponding eigenvalues $\delta_n + iv_n$, where $\delta_n = \omega_0 - \omega_n$ and v_n denote the collective line shift and linewidth, and ω_0 is the unshifted transition resonance frequency.

We engineer the spatially extended collective eigenmodes of a large array by designing the light-mediated interactions between the atoms in terms of the symmetries of an individual unit cell at each site that forms the lattice. Then the different eigenmodes of an appropriately chosen unit cell correspond to different multipole excitations, such as electric dipole, magnetic dipole, electric quadrupole, etc. Moreover, radiative interactions between atoms lead to collective eigenmodes of the entire array which behave as an effective lattice of unit cells, each with radiative properties determined by these multipole moments. Such eigenmodes can be excited by selectively manipulating each unit cell.

We consider first a square array of unit cells in the yz plane with lattice spacing d , where each unit cell consists of four atomic sites forming a square with side length a , as illustrated in Fig. 1(a). To characterize the optical response, we take the far-field radiation from each unit cell and decompose it into vector spherical harmonics [73]

$$\mathbf{E}_s^{(j)} = \sum_{l=0}^{\infty} \sum_{m=-l}^l (\alpha_{E,lm}^{(j)} \Psi_{lm} + \alpha_{B,lm}^{(j)} \Phi_{lm}). \quad (1)$$

This expansion allows a collection of point dipoles with different positions and orientations to be decomposed into a set of multipole moments at the origin [75], with Ψ_{lm} corresponding to an electric dipole \mathbf{d} for $l = 1$, quadrupole \mathbf{q}_e for $l = 2$, octopole for $l = 3$, etc., while Φ_{lm} represents magnetic multipoles (dipole \mathbf{m} , quadrupole \mathbf{q}_m , etc.).

To analyze the light-mediated interactions in a single unit cell which makes up the lattice, we take the eigenvectors \mathbf{v}_n of the matrix \mathcal{H} corresponding to these four atoms in

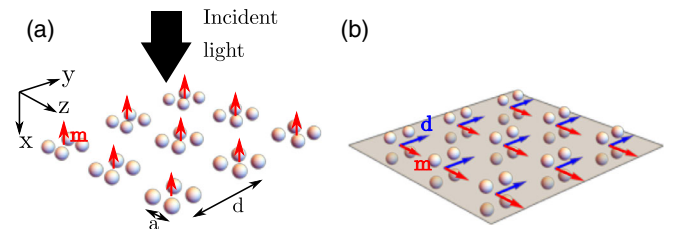


FIG. 1. (a) Array with square unit cells of lattice constant d and unit cell of size a to generate an array of magnetic dipoles pointing normal to the plane. (b) Bilayer array forming a Huygens' surface with crossed electric (\mathbf{d}) and magnetic (\mathbf{m}) dipoles.

TABLE I. Normalized multipole decomposition of the eigenmodes of a square unit cell with $a = 0.15\lambda$ and $\Delta_\sigma^{(j)} = 0$, as well as collective linewidths v_i^{uc} of each mode in an isolated unit cell and v_i in a 20×20 lattice of unit cells with $d = 0.5\lambda$. In 1–6 the polarization is in the yz plane while in 7–9 along the x direction. Degenerate modes are labeled with their degeneracy.

n	$ \mathbf{d} $	$ \mathbf{m} $	$ \mathbf{q}_e $	$ \mathbf{q}_m $	v_i^{uc}/γ	v_i/γ
1 ($\times 2$)	1				3.4	3.7
2		1			0.4	10^{-4}
3			1		0.25	10^{-3}
4			1		0.25	10^{-3}
5			1		0.08	10^{-3}
6 ($\times 2$)	0.89			0.05	0.09	0.1
7	1				3.3	0.02
8 ($\times 2$)		0.63	0.37		0.3	10^{-4}
9				0.78	0.02	10^{-8}

isolation, and decompose the scattered field for each of these eigenmodes. The results, normalized so that the sum of all multipole moments is one for each mode, are listed in Table I up to quadrupole moments, with the corresponding eigenmodes illustrated in Fig. S1 [73]. Most modes are dominantly represented by one of the multipole components and we find, e.g., eigenmodes with electric dipoles in the y or z ($n = 1$, doubly degenerate), or x ($n = 7$) directions. More interestingly, however, there are collective eigenmodes almost solely corresponding to a magnetic dipole in the x direction ($n = 2$) [inset of Fig. 2(b)], electric quadrupoles, and those dominated by magnetic quadrupoles.

The resonances of the electric dipole eigenmode (EDM) and magnetic dipole eigenmode (MDM) are only shifted by 3.8γ —on the order of the collective linewidth 3.4γ of the superradiant EDM (Table I). The MDM is subradiant

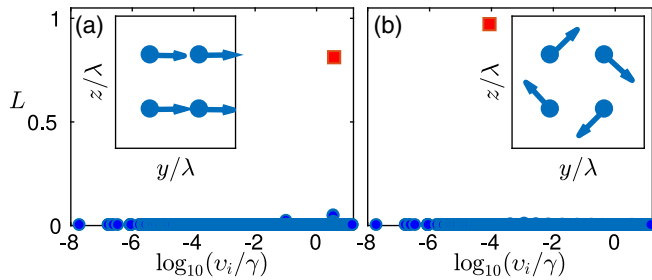


FIG. 2. (a) Occupations of collective excitation eigenmodes (ordered by linewidth v_i) in a steady state for a 20×20 ($\times 4$) array ($d = 0.5\lambda$, $a = 0.15\lambda$), shown in Fig. 1(a), illuminated by a Gaussian profile $\mathcal{E}_0(y, z)$ with $1/e^2$ radius 7λ , when detunings are optimized to target the collective eigenmode (red square) which is closest to a uniform repetition of the unit-cell electric dipole mode. (b) As in (a), but with a target magnetic dipole eigenmode closest to a uniform distribution of magnetic dipoles in the x direction (red square). Insets (a),(b): the resulting atomic dipoles on a central unit cell.

(linewidth $0.4\gamma < \gamma$). For each of these modes, there is a corresponding collective mode of the whole lattice which best resembles a uniform repetition of the eigenmode of each unit cell. The collective interacting nature of the eigenmodes in large arrays is most clearly manifested in the strongly subradiant response, with several of the modes having linewidths orders of magnitude narrower than that of a single atom, or an isolated unit cell.

The collective modes can be excited by varying the atomic level shifts within each unit cell, as illustrated in Fig. 2. We optimize the level shifts on each atom in the unit cell to maximize overlap with the desired mode, while keeping each unit cell identical. Targeting the EDM of Fig. 2(a) is straightforward with the incident field propagating along the x axis and linearly polarized along the y axis. The occupation measure of the collective eigenmode \mathbf{v}_j is defined as $L_j = |\mathbf{v}_j^T \mathbf{b}(t)|^2 / \sum_i |\mathbf{v}_i^T \mathbf{b}(t)|^2$ [23], with the resulting dominant occupation of the array-wide EDM closest to a uniform repetition of the unit-cell EDM. The central unit cell clearly shows the collective electric dipole moment [inset of Fig. 2(a)].

While the uniform collective EDM of the whole array is phase-matched with the incident light and is easy to excite, there is no direct coupling of the incident field to the uniform MDM. The MDM is also subradiant (dark) and difficult to excite. By choosing appropriate level shifts $\Delta_\sigma^{(j)}$ for individual atoms, we can break the symmetry, such that the EDM and MDM are no longer eigenmodes of the collective light-atom system of vanishing level shifts. The level shifts induce a coupling between the EDM and MDM, therefore exciting the MDM by first driving the EDM by the incident field, followed by the transfer of the excitation to the MDM. The process can be illustrated by an effective two-mode model between the two collective modes [73]

$$\partial_t \mathcal{P}_e = (i\delta_e + i\Delta - v_e) \mathcal{P}_e + \delta \mathcal{P}_m + f, \quad (2a)$$

$$\partial_t \mathcal{P}_m = (i\delta_m + i\Delta - v_m) \mathcal{P}_m + \delta \mathcal{P}_e, \quad (2b)$$

where $\mathcal{P}_{e,m}$ are the amplitudes, and $\delta_{e,m}$ and $v_{e,m}$ the collective resonance line shifts and linewidths of the EDM and MDM, respectively, and f denotes the incident-field driving that is only coupled to \mathcal{P}_e . The contribution of the alternating level shifts in a unit cell is encapsulated in δ [73] which induces a coupling between the modes. The alternating level shifts can be generated, e.g., by the ac Stark shifts of crossed standing waves [73].

The effective dynamics of Eq. (2) can represent both a single unit cell in isolation and the entire array of multiple unit cells. The two cases dramatically differ by the value of v_m that becomes strongly subradiant as the size of the array increases ($v_m \simeq 10^{-4}\gamma$ for a 20×20 array, Table I; see also Supplemental Material [73]). The ratio between the occupations of the MDM and EDM in the steady state of Eq. (2) at the resonance of the MDM is δ^2/v_m^2 . Therefore, the

narrow ν_m in large arrays allows the MDM to dramatically dominate the EDM, even for relatively small level splittings δ , providing a protocol for synthesizing a magnetic dipolar response that utilizes strong cooperative interactions in large systems. In other words, because of the deeply subradiant nature of the MDM, this excitation does not decay and becomes dominant in the steady state, in a process reminiscent of the electromagnetically induced transparency [77] of “dark” and “bright” states of non-interacting atoms. The excitation of the uniform collective MDM is shown in Fig. 2(b) with an occupation of ≈ 0.97 . For a single unit cell, the amplitude of the magnetic dipole radiation here is about 23% of that of a single atom, indicating strong optically active magnetism.

We next utilize the combination of electric and magnetic dipoles to prepare a Huygens’ surface. Huygens’ principle states each point on a propagating wave acts as a source of secondary spherical waves which interfere to produce the subsequent wavefront. A more rigorous formulation models each point as a perpendicular pair of electric and magnetic dipoles of equal strength [11,92]. Each such point then acts as an ideal point source for light which propagates only in the forward direction. While these secondary sources were originally introduced as a conceptual means to understand wave propagation, a physical implementation of such a surface consisting of real emitters can be used to engineer arbitrary wavefronts by controlling the phase of the light produced at each point.

To form an effective Huygens’ surface of crossed electric and magnetic dipoles we consider a geometry where each square unit cell is rotated around the y axis and lies in the xy plane, with the electric (magnetic) dipole in the y (z) direction [Fig. 1(b)]. This is equivalent to having a bilayer array with two sites per unit cell in each layer. We can again identify collective eigenmodes that are characterized by a uniform array of either electric and magnetic dipoles. In this case the collective linewidth of the MDM remains broader as the size of the array increases, since all the dipoles are in the same plane. We then control the atomic level shifts to form a superposition of the EDM and MDM on each unit cell.

To utilize the Huygens’ surface for wavefront engineering, we must control the phase of the total transmitted light at each unit cell, which consists of both the incident and scattered light [73]. We show the control of the phase over the whole range of $0 \leq \arg(\mathbf{E}) \leq 2\pi$ as a function of the detuning in an array of identical unit cells in Fig. 3(a), while the transmission remains above 90% at all points. Minimum transmission generally increases with the number of atoms, but is already over 80% for a 20×20 array. Note that spectrally nonoverlapping resonances of the EDM and MDM would produce significantly reduced transmission values at different frequencies. Having the two resonances spectrally overlapping yields a nearly flat line close to unity, despite providing a dramatic 2π phase

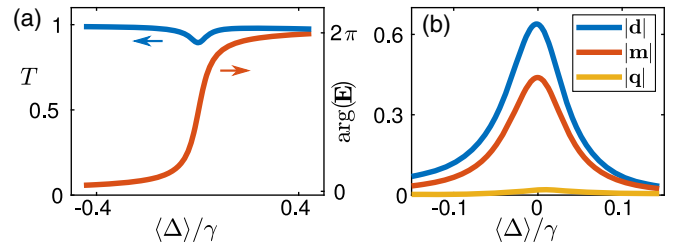


FIG. 3. (a) Transmission T (left axis) and phase (right axis) of the incident and scattered light in the forward direction as a function of the laser frequency for plane-wave illumination of a 32×32 lattice ($d = 0.8\lambda$, $a = 0.15\lambda$) showing the full 2π range with transmission everywhere exceeding 90%. (b) Decomposition of the corresponding radiative excitation into (curves from top to bottom) electric and magnetic dipole, and electric quadrupole contributions. The relative level shifts of all levels are held fixed, and identical on each unit cell.

change which is two times the phase shift that the magnetic or electric dipoles can individually contribute in resonance. The multipole decomposition of a unit cell at the center of the lattice is plotted in Fig 3(b), showing the combination of electric and magnetic dipoles. The results in Fig. 3 are achieved by controlling the level shifts and also allowing the positions of each atom in the unit cell to vary, up to a maximum of $0.05\lambda = a/3$, while keeping them constant from one unit cell to another.

We demonstrate wavefront engineering with the Huygens’ surface by transforming an ordinary input state with no OAM into an OAM state [73] or a superposition of OAM states, shown in Fig. 4 for $(|l=0\rangle + |l=1\rangle)/\sqrt{2}$, with the states of \hbar OAM per photon. In the single-photon limit, such entangled OAM states have applications to quantum information [63], and provide a larger alphabet $l = 0, \dots, N$ for quantum information architectures [64] than traditional two-state systems. We take the relative level shifts to be equal on all unit cells, while the overall shift varies such that the phase of the transmitted light gives the

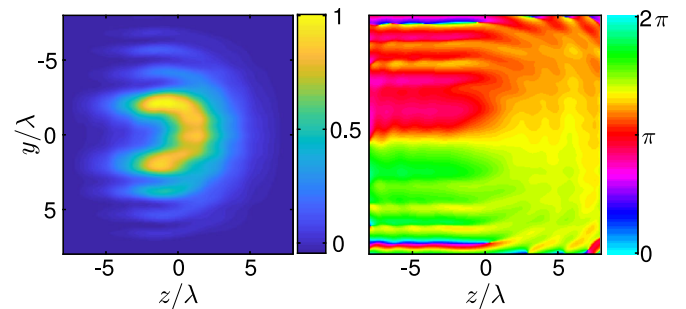


FIG. 4. (a) Transmitted intensity and (b) phase of the total electric field, calculated from each dipole at a distance 5λ for a 20×20 lattice ($d = 0.8\lambda$, $a = 0.15\lambda$) shown in Fig. 1(b). An incident Gaussian beam with waist $w_0 = 5\lambda$ is transformed into an equal superposition of states with orbital angular momentum 0 and \hbar per photon. The intensity varies with angle due to interference between the two components.

desired profile. Only 2% of the total power incident on the lattice is reflected backwards.

In conclusion, we showed how to harness light-mediated resonant dipole-dipole interactions in atomic arrays to design collective excitations that exhibit optically active magnetism and a Huygens' surface. This is achieved by first designing the interactions in an individual unit cell of the array to engineer a lattice of magnetic dipoles, or of crossed spectrally overlapping electric and magnetic dipoles. The latter can be used to create a nearly reflectionless Huygens' surface, consisting of ideal emitters with a fully 2π -controllable phase, that allows for arbitrary shaping of wavefronts, including even those for a single photon.

Data used in this publication is available at [94].

We acknowledge financial support from the UK Engineering and Physical Sciences Research Council (Grants No. EP/S002952/1, No. EP/P026133/1).

Note added.—Recently, we have become aware of a related parallel theoretical proposal on generating magnetic dipoles for atoms in Ref. [93].

*k.ballantine@lancaster.ac.uk

†j.ruostekoski@lancaster.ac.uk

- [1] L. D. Landau, E. M. Lifshitz, and L. P. Pitaevskii, *Electrodynamics of Continuous Media*, 2nd ed. (Pergamon Press, New York, 1984).
- [2] R. D. Cowan and University of California Press, *The Theory of Atomic Structure and Spectra*, Los Alamos Series in Basic and Applied Sciences (University of California Press, Berkeley, 1981).
- [3] N. I. Zheludev and Y. S. Kivshar, From metamaterials to metadevices, *Nat. Mater.* **11**, 917 (2012).
- [4] N. Yu and F. Capasso, Flat optics with designer metasurfaces, *Nat. Mater.* **13**, 139 (2014).
- [5] L. Novotny and B. Hecht, *Principles of Nano-Optics*, Principles of Nano-Optics (Cambridge University Press, Cambridge, England, 2012).
- [6] J. B. Pendry, Negative Refraction Makes a Perfect Lens, *Phys. Rev. Lett.* **85**, 3966 (2000).
- [7] J. B. Pendry, D. Schurig, and D. R. Smith, Controlling electromagnetic fields, *Science* **312**, 1780 (2006).
- [8] U. Leonhardt, Optical conformal mapping, *Science* **312**, 1777 (2006).
- [9] D. Schurig, J. J. Mock, B. J. Justice, S. A. Cummer, J. B. Pendry, A. F. Starr, and D. R. Smith, Metamaterial electromagnetic cloak at microwave frequencies, *Science* **314**, 977 (2006).
- [10] C. Huygens, *Traité de la lumière* (Leiden: Pieter van der Aa, 1690), https://archive.org/details/bub_gb_kVxsaYdZaa0C.
- [11] A. E. H. Love, The integration of the equations of propagation of electric waves, *Phil. Trans. R. Soc. A* **68**, 19 (1901), <https://www.jstor.org/stable/116514>.
- [12] C. Weitenberg, M. Endres, J. F. Sherson, M. Cheneau, P. Schauß, T. Fukuhara, I. Bloch, and S. Kuhr, Single-spin addressing in an atomic mott insulator, *Nature (London)* **471**, 319 (2011).
- [13] B. J. Lester, N. Luick, A. M. Kaufman, C. M. Reynolds, and C. A. Regal, Rapid Production of Uniformly Filled Arrays of Neutral Atoms, *Phys. Rev. Lett.* **115**, 073003 (2015).
- [14] T. Xia, M. Lichtman, K. Maller, A. W. Carr, M. J. Piotrowicz, L. Isenhower, and M. Saffman, Randomized Benchmarking of Single-Qubit Gates in a 2D Array of Neutral-Atom Qubits, *Phys. Rev. Lett.* **114**, 100503 (2015).
- [15] M. Endres, H. Bernien, A. Keesling, H. Levine, E. R. Anschuetz, A. Krajenbrink, C. Senko, V. Vuletic, M. Greiner, and M. D. Lukin, Atom-by-atom assembly of defect-free one-dimensional cold atom arrays, *Science* **354**, 1024 (2016).
- [16] D. Barredo, S. de Léséleuc, V. Lienhard, T. Lahaye, and A. Browaeys, An atom-by-atom assembler of defect-free arbitrary two-dimensional atomic arrays, *Science* **354**, 1021 (2016).
- [17] H. Kim, W. Lee, H.-G. Lee, H. Jo, Y. Song, and J. Ahn, In situ single-atom array synthesis using dynamic holographic optical tweezers, *Nat. Commun.* **7**, 13317 (2016).
- [18] A. Cooper, J. P. Covey, I. S. Madjarov, S. G. Porsev, M. S. Safronova, and M. Endres, Alkaline-Earth Atoms in Optical Tweezers, *Phys. Rev. X* **8**, 041055 (2018).
- [19] S. D. Jenkins and J. Ruostekoski, Controlled manipulation of light by cooperative response of atoms in an optical lattice, *Phys. Rev. A* **86**, 031602(R) (2012).
- [20] J. Perczel, J. Borregaard, D. E. Chang, H. Pichler, S. F. Yelin, P. Zoller, and M. D. Lukin, Photonic band structure of two-dimensional atomic lattices, *Phys. Rev. A* **96**, 063801 (2017).
- [21] R. J. Bettles, J. Minář, C. S. Adams, I. Lesanovsky, and B. Olmos, Topological properties of a dense atomic lattice gas, *Phys. Rev. A* **96**, 041603(R) (2017).
- [22] R. J. Bettles, S. A. Gardiner, and C. S. Adams, Enhanced Optical Cross Section via Collective Coupling of Atomic Dipoles in a 2D Array, *Phys. Rev. Lett.* **116**, 103602 (2016).
- [23] G. Facchinetti, S. D. Jenkins, and J. Ruostekoski, Storing Light with Subradiant Correlations in Arrays of Atoms, *Phys. Rev. Lett.* **117**, 243601 (2016).
- [24] G. Facchinetti and J. Ruostekoski, Interaction of light with planar lattices of atoms: Reflection, transmission, and cooperative magnetometry, *Phys. Rev. A* **97**, 023833 (2018).
- [25] E. Shahmoon, D. S. Wild, M. D. Lukin, and S. F. Yelin, Cooperative Resonances in Light Scattering from Two-Dimensional Atomic Arrays, *Phys. Rev. Lett.* **118**, 113601 (2017).
- [26] D. Plankensteiner, C. Sommer, H. Ritsch, and C. Genes, Cavity Antiresonance Spectroscopy of Dipole Coupled Subradiant Arrays, *Phys. Rev. Lett.* **119**, 093601 (2017).
- [27] A. Asenjo-Garcia, M. Moreno-Cardoner, A. Albrecht, H. J. Kimble, and D. E. Chang, Exponential Improvement in Photon Storage Fidelities Using Subradiance and Selective Radiances in Atomic Arrays, *Phys. Rev. X* **7**, 031024 (2017).
- [28] H. H. Jen, Phase-imprinted multiphoton subradiant states, *Phys. Rev. A* **96**, 023814 (2017).
- [29] P.-O. Guimond, A. Grankin, D. V. Vasilyev, B. Vermersch, and P. Zoller, Subradiant Bell States in Distant Atomic Arrays, *Phys. Rev. Lett.* **122**, 093601 (2019).

- [30] M. Hebenstreit, B. Kraus, L. Ostermann, and H. Ritsch, Subradiance via Entanglement in Atoms with Several Independent Decay Channels, *Phys. Rev. Lett.* **118**, 143602 (2017).
- [31] S. Krämer, L. Ostermann, and H. Ritsch, Optimized geometries for future generation optical lattice clocks, *Europhys. Lett.* **114**, 14003 (2016).
- [32] R. T. Sutherland and F. Robicheaux, Collective dipole-dipole interactions in an atomic array, *Phys. Rev. A* **94**, 013847 (2016).
- [33] S.-M. Yoo and S. M. Paik, Cooperative optical response of 2D dense lattices with strongly correlated dipoles, *Opt. Express* **24**, 2156 (2016).
- [34] Y.-X. Zhang and K. Mølmer, Theory of Subradiant States of a One-Dimensional Two-Level Atom Chain, *Phys. Rev. Lett.* **122**, 203605 (2019).
- [35] V. Mkhitarian, L. Meng, A. Marini, and F. J. de Abajo, Lasing and Amplification from Two-Dimensional Atom Arrays, *Phys. Rev. Lett.* **121**, 163602 (2018).
- [36] D. Bhatti, R. Schneider, S. Oettel, and J. von Zanthier, Directional Dicke Subradiance with Nonclassical and Classical Light Sources, *Phys. Rev. Lett.* **120**, 113603 (2018).
- [37] L. Henriot, J. S. Douglas, D. E. Chang, and A. Albrecht, Critical open-system dynamics in a one-dimensional optical-lattice clock, *Phys. Rev. A* **99**, 023802 (2019).
- [38] D. Plankensteiner, C. Sommer, M. Reitz, H. Ritsch, and C. Genes, Enhanced collective Purcell effect of coupled quantum emitter systems, *Phys. Rev. A* **99**, 043843 (2019).
- [39] J. Javanainen and R. Rajapakse, Light propagation in systems involving two-dimensional atomic lattices, *Phys. Rev. A* **100**, 013616 (2019).
- [40] R. J. Bettles, M. D. Lee, S. A. Gardiner, and J. Ruostekoski, Quantum and nonlinear effects in light transmitted through planar atomic arrays, *Commun. Phys.* **3**, 141 (2020).
- [41] C. Qu and A. M. Rey, Spin squeezing and many-body dipolar dynamics in optical lattice clocks, *Phys. Rev. A* **100**, 041602(R) (2019).
- [42] Y.-X. Zhang, C. Yu, and K. Mølmer, Subradiant bound dimer excited states of emitter chains coupled to a one dimensional waveguide, *Phys. Rev. Research* **2**, 013173 (2020).
- [43] E. Shahmoon, M. D. Lukin, and S. F. Yelin, Collective motion of an atom array under laser illumination, *Adv. At. Mol. Opt. Phys.* **68**, 1 (2019).
- [44] F. Lemoult, G. Lerosey, J. de Rosny, and M. Fink, Resonant Metalenses for Breaking the Diffraction Barrier, *Phys. Rev. Lett.* **104**, 203901 (2010).
- [45] S. D. Jenkins, J. Ruostekoski, N. Papisimakis, S. Savo, and N. I. Zheludev, Many-Body Subradiant Excitations in Metamaterial Arrays: Experiment and Theory, *Phys. Rev. Lett.* **119**, 053901 (2017).
- [46] A. Grankin, P. O. Guimond, D. V. Vasilyev, B. Vermersch, and P. Zoller, Free-space photonic quantum link and chiral quantum optics, *Phys. Rev. A* **98**, 043825 (2018).
- [47] K. E. Ballantine and J. Ruostekoski, Subradiance-protected excitation spreading in the generation of collimated photon emission from an atomic array, *Phys. Rev. Research* **2**, 023086 (2020).
- [48] S. Balik, A. L. Win, M. D. Havey, I. M. Sokolov, and D. V. Kupriyanov, Near-resonance light scattering from a high-density ultracold atomic ^{87}Rb gas, *Phys. Rev. A* **87**, 053817 (2013).
- [49] J. Chabé, M.-T. Rouabah, L. Bellando, T. Bienaimé, N. Piovella, R. Bachelard, and R. Kaiser, Coherent and incoherent multiple scattering, *Phys. Rev. A* **89**, 043833 (2014).
- [50] J. Pellegrino, R. Bourgain, S. Jennewein, Y. R. P. Sortais, A. Browaeys, S. D. Jenkins, and J. Ruostekoski, Observation of Suppression of Light Scattering Induced by Dipole-Dipole Interactions in a Cold-Atom Ensemble, *Phys. Rev. Lett.* **113**, 133602 (2014).
- [51] A. S. Sheremet, I. M. Sokolov, D. V. Kupriyanov, S. Balik, A. L. Win, and M. D. Havey, Light scattering on the $F = 1 \rightarrow F' = 0$ transition in a cold and high density ^{87}Rb vapor, *J. Mod. Opt.* **61**, 77 (2014).
- [52] C. C. Kwong, T. Yang, M. S. Pramod, K. Pandey, D. Delande, R. Pierrat, and D. Wilkowski, Cooperative Emission of a Coherent Superflash of Light, *Phys. Rev. Lett.* **113**, 223601 (2014).
- [53] S. Jennewein, M. Besbes, N. J. Schilder, S. D. Jenkins, C. Sauvan, J. Ruostekoski, J.-J. Greffet, Y. R. P. Sortais, and A. Browaeys, Coherent Scattering of Near-Resonant Light by a Dense Microscopic Cold Atomic Cloud, *Phys. Rev. Lett.* **116**, 233601 (2016).
- [54] S. L. Bromley, B. Zhu, M. Bishof, X. Zhang, T. Bothwell, J. Schachenmayer, T. L. Nicholson, R. Kaiser, S. F. Yelin, M. D. Lukin, A. M. Rey, and J. Ye, Collective atomic scattering and motional effects in a dense coherent medium, *Nat. Commun.* **7**, 11039 (2016).
- [55] S. D. Jenkins, J. Ruostekoski, J. Javanainen, R. Bourgain, S. Jennewein, Y. R. P. Sortais, and A. Browaeys, Optical Resonance Shifts in the Fluorescence of Thermal and Cold Atomic Gases, *Phys. Rev. Lett.* **116**, 183601 (2016).
- [56] P. C. Bons, R. de Haas, D. de Jong, A. Groot, and P. van der Straten, Quantum Enhancement of the Index of Refraction in a Bose-Einstein Condensate, *Phys. Rev. Lett.* **116**, 173602 (2016).
- [57] W. Guerin, M. O. Araújo, and R. Kaiser, Subradiance in a Large Cloud of Cold Atoms, *Phys. Rev. Lett.* **116**, 083601 (2016).
- [58] S. Machluf, J. B. Naber, M. L. Soudijn, J. Ruostekoski, and R. J. C. Spreeuw, Collective suppression of optical hyperfine pumping in dense clouds of atoms in microtraps, *Phys. Rev. A* **100**, 051801(R) (2019).
- [59] L. Corman, J. L. Ville, R. Saint-Jalm, M. Aidelsburger, T. Bienaimé, S. Nascimbène, J. Dalibard, and J. Beugnon, Transmission of near-resonant light through a dense slab of cold atoms, *Phys. Rev. A* **96**, 053629 (2017).
- [60] R. J. Bettles, T. Ilieva, H. Busche, P. Huillery, S. W. Ball, N. L. R. Spong, and C. S. Adams, Collective mode interferences in light-matter interactions, [arXiv:1808.08415](https://arxiv.org/abs/1808.08415).
- [61] R. Saint-Jalm, M. Aidelsburger, J. L. Ville, L. Corman, Z. Hadzibabic, D. Delande, S. Nascimbène, N. Cherroret, J. Dalibard, and J. Beugnon, Resonant-light diffusion in a disordered atomic layer, *Phys. Rev. A* **97**, 061801(R) (2018).
- [62] J. Rui, D. Wei, A. Rubio-Abadal, S. Hollerith, J. Zeiher, D. M. Stamper-Kurn, C. Gross, and I. Bloch, A subradiant

- optical mirror formed by a single structured atomic layer, *Nature (London)* **583**, 369 (2020).
- [63] A. Mair, A. Vaziri, G. Weihs, and A. Zeilinger, Entanglement of the orbital angular momentum states of photons, *Nature (London)* **412**, 313 (2001).
- [64] H. Bechmann-Pasquinucci and W. Tittel, Quantum cryptography using larger alphabets, *Phys. Rev. A* **61**, 062308 (2000).
- [65] C. Pfeiffer and A. Grbic, Metamaterial Huygens' Surfaces: Tailoring Wave Fronts with Reflectionless Sheets, *Phys. Rev. Lett.* **110**, 197401 (2013).
- [66] M. Decker, I. Staude, M. Falkner, J. Dominguez, D. N. Neshev, I. Brener, T. Pertsch, and Y. S. Kivshar, High-efficiency dielectric huygens surfaces, *Adv. Opt. Mater.* **3**, 813 (2015).
- [67] Y. F. Yu, A. Y. Zhu, R. Paniagua-Domnguez, Y. H. Fu, B. Luk'yanchuk, and A. I. Kuznetsov, High-transmission dielectric metasurface with 2π phase control at visible wavelengths, *Laser Photonics Rev.* **9**, 412 (2015).
- [68] K. E. Chong, I. Staude, A. James, J. Dominguez, S. Liu, S. Campione, G. S. Subramania, T. S. Luk, M. Decker, D. N. Neshev, I. Brener, and Y. S. Kivshar, Polarization-independent silicon metadevices for efficient optical wavefront control, *Nano Lett.* **15**, 5369 (2015).
- [69] M. I. Shalaev, J. Sun, A. Tsukernik, A. Pandey, K. Nikolskiy, and N. M. Litchinitser, High-efficiency all-dielectric metasurfaces for ultracompact beam manipulation in transmission mode, *Nano Lett.* **15**, 6261 (2015).
- [70] S. S. Kruk, Z. J. Wong, E. Pshenay-Severin, K. O'Brien, D. N. Neshev, Y. S. Kivshar, and X. Zhang, Magnetic hyperbolic optical metamaterials, *Nat. Commun.* **7**, 11329 (2016).
- [71] R. Paniagua-Domínguez, Y. F. Yu, A. E. Miroshnichenko, L. A. Krivitsky, Y. H. Fu, V. Valuckas, L. Gonzaga, Y. T. Toh, A. Y. S. Kay, B. Luk'yanchuk, and A. I. Kuznetsov, Generalized brewster effect in dielectric metasurfaces, *Nat. Commun.* **7**, 10362 (2016).
- [72] F. Gerbier, A. Widera, S. Fölling, O. Mandel, and I. Bloch, Resonant control of spin dynamics in ultracold quantum gases by microwave dressing, *Phys. Rev. A* **73**, 041602(R) (2006).
- [73] See Supplemental Material at <http://link.aps.org/supplemental/10.1103/PhysRevLett.125.143604> for technical details, which includes Refs. [19,23,24,39,74–83].
- [74] M. D. Lee, S. D. Jenkins, and J. Ruostekoski, Stochastic methods for light propagation and recurrent scattering in saturated and nonsaturated atomic ensembles, *Phys. Rev. A* **93**, 063803 (2016).
- [75] J. D. Jackson, *Classical Electrodynamics*, 3rd ed. (Wiley, New York, 1999).
- [76] S. D. Jenkins, J. Ruostekoski, J. Javanainen, S. Jennewein, R. Bourgain, J. Pellegrino, Y. R. P. Sortais, and A. Browaeys, Collective resonance fluorescence in small and dense atom clouds: Comparison between theory and experiment, *Phys. Rev. A* **94**, 023842 (2016).
- [77] M. Fleischhauer, A. Imamoglu, and J. P. Marangos, Electromagnetically induced transparency: Optics in coherent media, *Rev. Mod. Phys.* **77**, 633 (2005).
- [78] B. Olmos, D. Yu, Y. Singh, F. Schreck, K. Bongs, and I. Lesanovsky, Long-Range Interacting Many-Body Systems with Alkaline-Earth-Metal Atoms, *Phys. Rev. Lett.* **110**, 143602 (2013).
- [79] O. Mandel, M. Greiner, A. Widera, T. Rom, T. W. Hänsch, and I. Bloch, Controlled collisions for multi-particle entanglement of optically trapped atoms, *Nature (London)* **425**, 937 (2003).
- [80] L. Chomaz, L. Corman, T. Yefsah, R. Desbuquois, and J. Dalibard, Absorption imaging of a quasi-two-dimensional gas: A multiple scattering analysis, *New J. Phys.* **14**, 055001 (2012).
- [81] J. Javanainen, J. Ruostekoski, Y. Li, and S.-M. Yoo, Exact electrodynamics versus standard optics for a slab of cold dense gas, *Phys. Rev. A* **96**, 033835 (2017).
- [82] L. Allen, S. M. Barnett, and M. J. Padgett, *Optical Angular Momentum*, Optics & Optoelectronics (Taylor & Francis, London, 2003).
- [83] A. A. Svidzinsky, J.-T. Chang, and M. O. Scully, Cooperative spontaneous emission of n atoms: Many-body eigenstates, the effect of virtual Lamb shift processes, and analogy with radiation of n classical oscillators, *Phys. Rev. A* **81**, 053821 (2010).
- [84] J. A. Needham, I. Lesanovsky, and B. Olmos, Subradiance-protected excitation transport, *New J. Phys.* **21**, 073061 (2019).
- [85] O. Morice, Y. Castin, and J. Dalibard, Refractive index of a dilute bose gas, *Phys. Rev. A* **51**, 3896 (1995).
- [86] J. Ruostekoski and J. Javanainen, Quantum field theory of cooperative atom response: Low light intensity, *Phys. Rev. A* **55**, 513 (1997).
- [87] J. Javanainen, J. Ruostekoski, B. Vestergaard, and M. R. Francis, One-dimensional modeling of light propagation in dense and degenerate samples, *Phys. Rev. A* **59**, 649 (1999).
- [88] I. M. Sokolov, D. V. Kupriyanov, and M. D. Havey, Microscopic theory of scattering of weak electromagnetic radiation by a dense ensemble of ultracold atoms, *J. Exp. Theor. Phys.* **112**, 246 (2011).
- [89] J. Javanainen, J. Ruostekoski, Y. Li, and S.-M. Yoo, Shifts of a Resonance Line in a Dense Atomic Sample, *Phys. Rev. Lett.* **112**, 113603 (2014).
- [90] R. T. Sutherland and F. Robicheaux, Coherent forward broadening in cold atom clouds, *Phys. Rev. A* **93**, 023407 (2016).
- [91] The light and atomic field amplitudes here refer to the slowly varying positive frequency components, where the rapid oscillations $\exp(-i\omega t)$ at the laser frequency have been factored out.
- [92] S. A. Schelkunoff, Some equivalence theorems of electromagnetics and their application to radiation problems, *Bell Syst. Tech. J.* **15**, 92 (1936).
- [93] R. Alaee, B. Gurlek, M. Albooyeh, D. Martín-Cano, and V. Sandoghdar, Quantum Metamaterials with Magnetic Response at Optical Frequencies, *Phys. Rev. Lett.* **125**, 063601 (2020).
- [94] <https://doi.org/10.17635/lancaster/researchdata/383>.